Are your MRI contrast agents cost-effective?
Learn more about generic Gadolinium-Based Contrast Agents.
FRESENIUS KABI
caring for life

AJNR

Neonatal Hypoxic-ischemic Encephalopathy: Detection with Diffusion-weighted MR Imaging

Kirsten P. N. Forbes, James G. Pipe and Roger Bird

AJNR Am J Neuroradiol 2000, 21 (8) 1490-1496
http://www.ajnr.org/content/21/8/1490

This information is current as of April 19, 2024.

AJNR Am J Neuroradiol 21:1490–1496, September 2000

Neonatal Hypoxic-ischemic Encephalopathy: Detection with Diffusion-weighted MR Imaging

Kirsten P. N. Forbes, James G. Pipe, and Roger Bird

BACKGROUND AND PURPOSE: **Although diffusion-weighted imaging has been shown to be highly sensitive in detecting acute cerebral infarction in adults, its use in detecting neonatal hypoxic-ischemic encephalopathy (HIE) has not been fully assessed. We examined the ability of this technique to detect cerebral changes of acute neonatal HIE in different brain locations.**

METHODS: **Fifteen MR examinations were performed in 14 neonates with HIE (median age, 6.5 days; range, 2–11 days). Imaging comprised conventional T1-weighted, proton density–weighted, and T2-weighted sequences and echo-planar diffusion-weighted sequences. The location, extent, and image timing of ischemic damage on conventional and diffusion-weighted sequences and apparent diffusion coefficient (ADC) maps were compared.**

RESULTS: **Although conventional sequences showed cerebral changes consistent with ischemia on all examinations, diffusion-weighted imaging showed signal hyperintensity associated with decreased ADC values in only seven subjects (47%). All subjects with isolated cortical infarction on conventional sequences had corresponding hyperintensity on diffusion-weighted images and decreased ADC values, as compared with 14% of subjects with deep gray matter/perirolandic cortical damage. The timing of imaging did not significantly alter diffusion-weighted imaging findings.**

CONCLUSION: **Diffusion-weighted imaging, performed with the technical parameters in this study, may have a lower correlation with clinical evidence of HIE than does conventional MR imaging. The sensitivity of diffusion-weighted imaging in detecting neonatal HIE appears to be affected by the pattern of ischemic damage, with a lower sensitivity if the deep gray matter is affected as compared with isolated cerebral cortex involvement.**

Early diagnosis of hypoxic-ischemic encephalopathy (HIE) is particularly important in the immediate postnatal period, when decisions about the provision of active life support must be made. Clinical confirmation of ischemic damage is often difficult at this time, when the neonate may present with nonspecific clinical features, such as seizures, hypotonia, or lethargy (1).

Diffusion-weighted imaging has proved more sensitive than conventional MR imaging sequences in detecting acute cerebral infarction in adult subjects (2). This technique can detect parenchymal changes associated with potentially severe cellular damage within minutes of severe ischemia (3). In adults, the size and intensity of the imaging alteration commonly peak about 48 hours after the insult (4, 5), and may remain visible for up to 10 to 14 days (6, 7).

Received October 14, 1999; accepted after revision March 1, 2000.

From the Division of Neuroradiology, Barrow Neurological Institute, St. Joseph's Hospital and Medical Center, 350 W Thomas Rd, Phoenix, AZ 85013. Address reprint requests to Kirsten Forbes, MRCP, FRCR.

The successful use of diffusion-weighted imaging in adults has led to several recent studies examining its use in neonates (8–11). While the technique appears sensitive to focal neonatal infarction, there is concern that it may either underestimate or fail to detect some global hypoxic-ischemic injuries (9). We postulated that the sensitivity of diffusion-weighted imaging might be affected by the pattern of brain injury. To assess this hypothesis, we applied a scoring system for neonatal hypoxic-ischemic damage (12) detected by diffusion-weighted and conventional MR imaging.

Methods

We retrospectively identified 14 neonates with HIE who were born within a 2-year period (1996–1998) at our institution. Subjects were identified by using a radiologic database and were included in the study if clinical records showed perinatal asphyxia and subsequent HIE. All subjects underwent both conventional and diffusion-weighted MR imaging of the brain during the first 11 days of life (mean age, 6.7 days). One subject was imaged on two separate occasions, leading to a total of 15 examinations.

TABLE 1: Clinical findings

Subject No.	Gestation (wk)	Signs of Fetal Distress	Delivery Method	Weight (g)	APGAR 0, 5, 10 min	ABG	Neurologic Findings
1	40	NFM 2 days, MSAF, late decelerations	ECS	2925	4, 6, · · ·	· · ·	Seizures at 24 hr, hypotonic
2	40	MSAF, bradycardia	IVD	· · ·	3, 5, · · ·	6.6	Seizures at 1 hr, irritability
3	39	NFM 2 days, MSAF, prolapsed cord	ECS	2520	5, 9, · · ·	7.1	Seizures, irritability
4	38	MSAF, bradycardia, late decelerations	IVD	· · ·	4, 6, · · ·	· · ·	Seizures, hypotonia
5	39	Placental abruption, bradycardia	ECS	2885	1, 7, · · ·	6.6	Status epilepticus 10 min after birth
6	37	Prolapsed cord, bradycardia	ECS	2765	1, 4, · · ·	· · ·	Seizures at 1 hr
7	40	Placental abruption, bradycardia	ECS	2720	0, 2, 5	7.0	Seizures 15 min after birth
8	38	Uterine rupture during TOL, bradycardia	ECS	3525	1, 4, · · ·	6.7	Seizures, autonomic dysfunction
9	40	Bradycardia	ECS	3690	· · ·	7.0	Seizures within minutes after birth
10	41	Placental abruption, MSAF	ECS	· · ·	0, 0, 0	6.8	Seizures within minutes after birth
11	39	Placental abruption, bradycardia	ECS	3405	0, 0, 0	6.9	Tremor, posturing
12	42	MSAF, bradycardia	IVD	3295	2, 4, 7	7.0	Seizures at 1 hr
13	40	MSAF, absent HRV	IVD	· · ·	2, 5, · · ·	· · ·	Seizures, jittery at birth
14	36	Placenta previa, bradycardia	ECS	3090	0, 1, · · ·	· · ·	Seizures

Note.—NFM indicates no fetal movement; MSAF, meconium-stained amniotic fluid; HRV, heart rate variability; TOL, trial of labor; ECS, emergency cesarean section; IVD, induced vaginal delivery; ABG, arterial blood gas.

Clinical Features

The clinical and laboratory features suggesting the diagnosis of perinatal asphyxia are shown in Table 1. All subjects except four (cases 1, 3, 6, and 14) presented during labor, with signs of fetal distress resulting in either immediate cesarean section or rapid vaginal delivery. Subjects 1 and 3 showed no fetal movement for the 2 days preceding delivery, subject 6 presented with a prolonged prolapsed cord, and subject 14 showed fetal distress after maternal vaginal bleeding. Subjects were considered to have HIE if they showed the clinical signs described by Sarnat and Sarnat (13). The individual neurologic findings shown in Table 1 were all observed during the first day of life, with exact times shown, where available. On the basis of information obtained from the clinical records, we judged 13 subjects to have Sarnat and Sarnat grade 2 HIE, marked by seizure activity, hypotonia, and lethargy. Subject 8 was thought to have grade 3 HIE, reflecting a severe encephalopathy with frequent seizures, flaccid weakness, stupor, and autonomic dysfunction.

In addition to the neurologic findings listed, nine subjects (cases 1, 4–8, 10, 11, and 13) suffered respiratory compromise or failure, and four subjects (cases 7, 9, 11, and 12) had suspected, although unconfirmed, sepsis. Subject 7 had severe anemia of uncertain origin.

The final discharge diagnosis for all subjects was HIE secondary to perinatal asphyxia. Clinical follow-up was available for five subjects, all of whom showed persistent neurologic deficits. Subject 1 had seizures at 1 year; subject 2 had diffuse hypertonia, mental retardation, and seizures at 2 years; subject 5 had persistent muscular spasms at 10 months; subject 6 had dyskinetic cerebral palsy at 23 months; and subject 13 had spastic quadriparesis at 26 months. Subject 7 died on day 4 of life; there was no postmortem examination.

Imaging Parameters

Sequential conventional and diffusion-weighted MR imaging studies were performed on a 1.5-T unit. Conventional spin-echo MR imaging comprised axial (TR/TE/excitations 480/16/1) and sagittal (450/8/1) T1-weighted sequences and axial T2-weighted sequences (3000/30–90/1). Imaging parameters were as follows: slice thickness, 4 mm; interslice gap, 2 mm; field of view, 18 to 20 cm; matrix size, 256 × 192. An echo-planar technique was used for diffusion-weighted imaging, with a maximum diffusion-sensitizing gradient strength of 1000 s/mm^2 applied to three orthogonal planes. A T2-weighted sequence was obtained in the absence of the diffusion-sensitizing gradient. The following imaging parameters were applied: 6500/101/1; slice thickness, 5 mm; interslice gap, 2.5 mm; field of view, 20 cm; matrix size, 128 × 128.

Apparent diffusion coefficient (ADC) maps were generated for all examinations using the Stejskal and Tanner equation (14): $S\ S_o e^{-bADC}$, where S signal intensity when the maximum diffusion sensitizing gradient, b, is applied and S_o signal intensity without the diffusion gradient.

Image Analysis

Images were assessed for the presence of ischemic damage by an experienced pediatric neuroradiologist. Although a history of HIE was given for all subjects, more detailed clinical information was not released. Diffusion-weighted images were examined before, and without knowledge of, the conventional MR findings. The three anisotropic diffusion images were examined for signal hyperintensity not accounted for by normal white matter anisotropy. Although the T2-weighted echo-planar image was also available for diffusion-weighted imaging interpretation, no attempt was made to assess whether signal hyperintensity was due to decreased water diffusion or to the effects of T2 shine-through. Conventional MR studies were later examined for the characteristic MR findings of HIE (15) without knowledge of the diffusion-weighted imaging appearances. The location of ischemic damage on each sequence was recorded using a scoring system for neonatal HIE (Table 2) (12).

Mean ADC values (± SD) were derived from isotropic ADC maps in three standard locations for each subject. Bilateral regions of interest were manually drawn around the lateral

TABLE 2: Basal ganglia/watershed scoring system

MR Imaging Findings	Score
Normal	0
Abnormal signal in basal ganglia or thalamus	1
Abnormal signal in cortex	2
Abnormal signal in cortex and basal nuclei (basal ganglia or thalami)	3
Abnormal signal in entire cortex and basal nuclei	4

Note.—From Barkovich et al. (12).

thalami (mean number of pixels, five), dorsilateral putamina (mean number of pixels, four), and anterior and posterior subcortical watershed areas (mean number of pixels, 18), and mean ADCs were calculated. Separate regions of interest were also drawn within regions of hyperintensity on diffusion-weighted images, and the enclosed ADC was calculated. Results were compared with published normal values (16), and the percentage of ADC change was calculated.

Data were analyzed with respect to both injury location and image timing. The full extent of ischemic damage in each subject was determined by using information from both conventional MR findings and ADC values. Areas of presumed damage showed either conventional MR signal changes or a low ADC value, or both. The ability of each imaging technique to detect the full extent of ischemic damage was assessed. The effect of image timing on the ability of diffusion-weighted imaging to detect ischemic damage was considered for all examinations and also separately for deep gray matter and cortical injuries.

Results

The results from conventional and diffusion-weighted MR imaging and ADC mapping are summarized in Table 3. Ischemic damage to the brain parenchyma was confirmed in all 15 studies. The full extent of ischemic injury was demonstrated by conventional MR imaging in 13 cases, with two studies showing additional areas of reduced ADC, suggesting ischemic damage (subjects 12 [day 4] and 13). Ischemic damage was detected on diffusion-weighted images and confirmed by a reduced ADC in seven subjects (47%). The full extent of injury was seen on diffusion-weighted images in only five subjects (cases 1–4 and 13).

Injury Location

Solitary cortical injuries (score 2) were equally well detected by conventional MR imaging, diffusion-weighted imaging, and ADC quantification (Fig 1). Follow-up conventional MR imaging was performed in subject 4 at 10 months, confirming permanent ischemic damage at the site of initial injury.

Conventional MR imaging detected the full extent of all injuries affecting the deep gray matter and perirolandic cortex (score 3), while diffusion-weighted imaging showed normal findings in five subjects (Fig 2): it did detect part of the injury in subjects 5 (perirolandic cortex) and 8 (dorsilateral putamina). Although the ADC was decreased at this location in subject 5 (0.50 ± 0.05; mean $\pm$ SD), it was increased in subject 8 (1.43 ± 0.21). This finding, together with corresponding T2 signal

TABLE 3: Imaging findings according to site of ischemic damage

Subject No.	Age (d)	Conventional MR Imaging Score	Diffusion-Weighted Imaging Score	ADC Change	Maximum ADC Change (%)
Score 2					
1	3	2	2	Decrease in anterior/posterior watershed zones	−53
2	4	2	2	Focal decrease in left parietal lobe	−60
3	5	2	2	Decrease in posterior watershed zones	−38
4	6	2	2	Decrease in anterior/posterior watershed zones	−52
Score 3					
5	2	3	2	Decrease in thalmi, putamina, and perirolandic cortex	−65
6	4	3	0	Normal	0
7	6	3	0	Normal	0
8	7	3	1	Increase in thalami and putamina	+25
9	8	3	0	Normal	0
10	10	3	0	Increase in thalami and putamina	+13
11	11	3	0	Increase in thalami and putamina	+10
Score 4					
12	4	1	0	Decrease in thalami, putamina, and anterior/posterior watershed zones	−50
12	11	4	4	Decrease in thalami and putamina; normal cortex	−44
13	9	2	2	Decrease in putamina and anterior/posterior watershed zones	−50
Periventricular white matter					
14	10	NA	0	Normal	0

Note.—ADC indicates apparent diffusion coefficient; NA, not applicable.

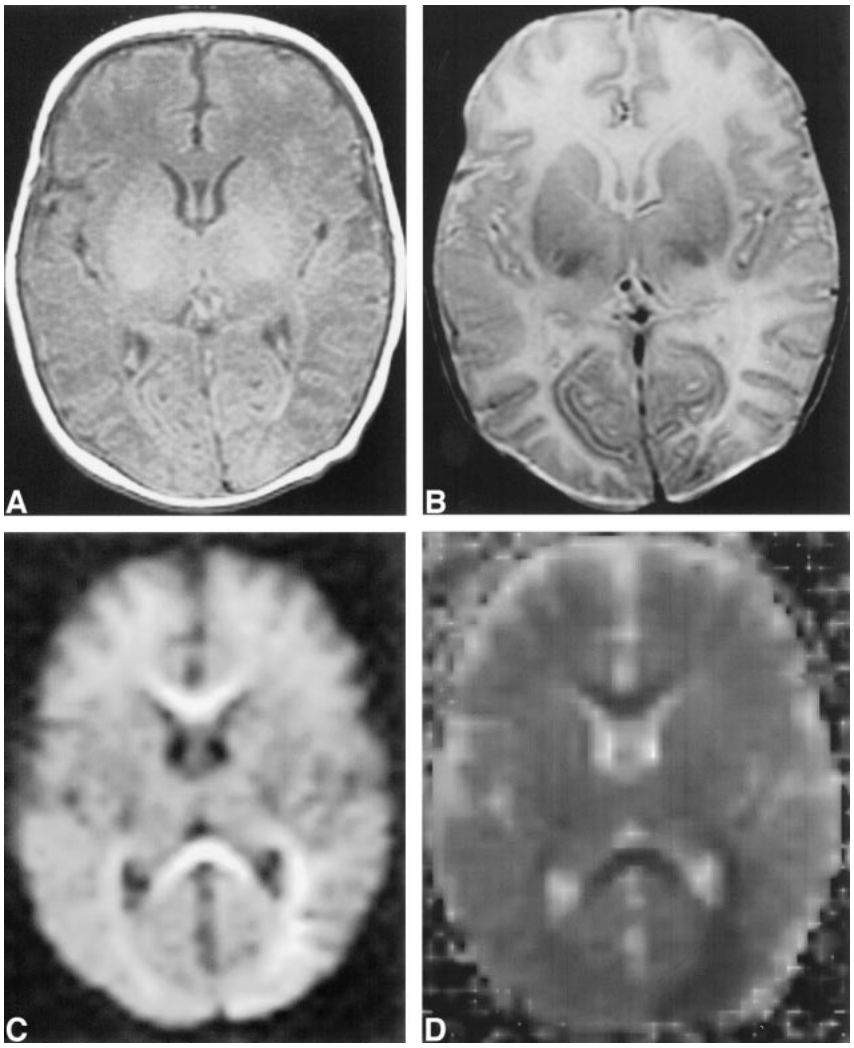

FIG 1. Subject 4: watershed ischemia.

A, T1-weighted image shows hypointensity bilaterally in the anterior and posterior watershed areas.

B, T2-weighted image shows hyperintensity in the same areas, suggesting edema.

C, Anisotropic diffusion-weighted image (*z* gradient) shows corresponding signal hyperintensity.

D, Isotropic ADC map confirms a decrease in water diffusion with hypointensity in all watershed regions, most prominently seen in left posterior watershed area.

hyperintensity, suggested T2 shine-through in subject 8. Diffusion-weighted imaging was significantly better at detecting score 2 injury as compared with score 3 injury, which was confirmed by reduced ADC values (χ^2 test, $P < .05$).

Widespread brain injuries (score 4) were not fully demonstrated by any one imaging method. Diffusion-weighted images were interpreted as normal at day 4 in subject 12, despite reduced ADC in the deep gray matter (0.55 ± 0.07) and watershed areas (0.72 ± 0.08). Similarly, despite showing cortical damage in subject 13, diffusion-weighted images did not show an ADC decrease in the putamina (0.64 ± 0.13). This was confirmed as ischemic damage on follow-up conventional MR studies 2 years later.

Image Timing

The median age of subjects at the time of MR imaging was 6.5 days (range, 2–11 days). In general, those neonates who showed areas of reduced ADC were younger at imaging, with a median age of 5.5 days (range, 2–11 days). Subjects who had normal ADC values were imaged at a median age of 7 days (range, 4–10 days), and those with areas of ADC increase were slightly older at the time of imaging, with a median age of 9.3 days (range, 7–11 days). Differences in age were not statistically significant.

We examined the effect of image timing on ADC values in different locations of ischemic damage. The ADC values in areas of cortical damage (scores 2 and 4) are shown in Figure 3, and thalamic values (scores 3 and 4) are shown in Figure 4. The change in ADC in isolated cortical injury (Fig 3) appears to be similar to the pattern observed in adult cerebral infarction. A decrease in ADC is seen after injury, with values returning to normal toward day 11. There appears to be a slightly different trend for areas of thalamic injury (Fig 4). After an initial decrease in ADC, values appear to rise more quickly up toward normal or mildly elevated levels. However, low ADC values were seen in two subjects at days 9 and 11, respectively.

Discussion

Our results demonstrate that diffusion-weighted imaging can detect parenchymal changes from se-

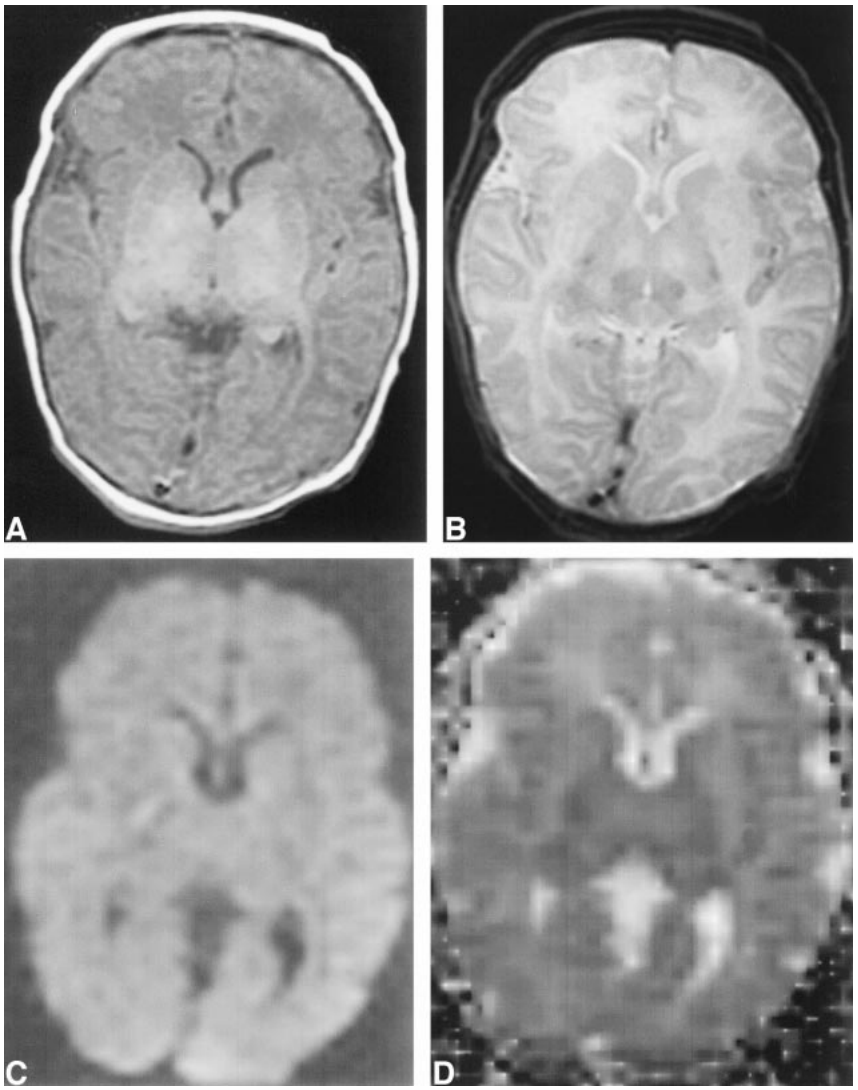

FIG 2. Subject 10: deep gray matter ischemia.

A and *B*, T1-weighted (*A*) and T2-weighted (*B*) images show hyperintensity in the thalami and lentiform nuclei.

C and *D*, Anisotropic diffusion-weighted image (*z* gradient) (*C*) and isotropic ADC map (*D*) confirm normal water diffusion.

vere cerebral ischemia in fewer than 50% of neonates with clinical evidence of HIE. Although controversy remains as to the exact cellular mechanism that increases diffusion-weighted imaging signal after severe ischemia, it is thought to be at least in part due to cellular swelling, or cytotoxic edema (3). In response to reduced arterial flow, the function of the Na^+-K^+-ATPase pump declines, leading to an influx of sodium, calcium, and water into the cell. Since water in the extracellular space shows

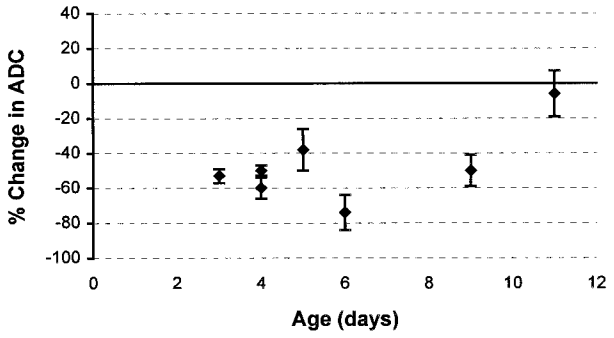

FIG 3. Cortical injuries: correlation between image timing and ADC changes. The age of each subject with cortical ischemic damage is shown. ADC changes within the ischemic region were calculated using normal published values (16), with error bars shown (SD). All subjects except case 12 (day 11) had a significant decrease in ADC values.

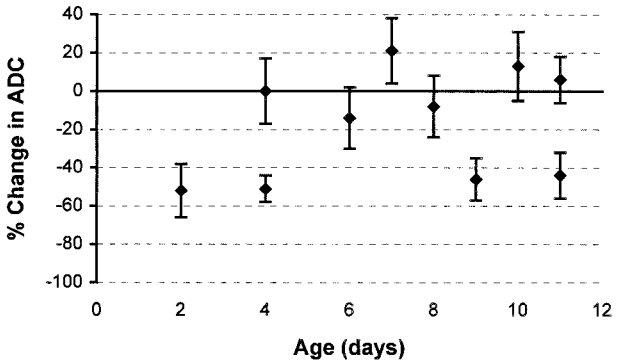

FIG 4. Thalamic injuries: correlation between image timing and ADC changes. The age of each subject with thalamic ischemic damage is shown. Four imaging studies show a significant decrease in ADC: subjects 5 (day 2); 12 (days 4 and 11), and 13 (day 9).

more random water diffusion than that in the restricted intracellular space, these changes in water balance result in a decrease in focal tissue diffusion. Diffusion-weighted imaging can detect this decrease in water diffusion, which is shown as an area of increased signal. Quantification of ADC can both confirm this decrease and remove erroneous interpretation arising from T2 shine-through or poor diffusion-weighted imaging windowing.

Whereas the sensitivity of diffusion-weighted imaging to adult cerebral infarction is 88% to 99% (2, 17), our results suggest that this technique is much less sensitive to neonatal HIE. There is good acute evidence that all subjects in this study suffered HIE, with follow-up studies, where available, supporting this. We have assumed that ischemic injuries in all cases occurred around the time of birth. While the presence of prenatal fetal distress and postnatal clinical and laboratory findings show this assumption to be likely, it remains possible that ischemia may have occurred in some of our subjects several days before birth, leading to an erroneously negative result.

Differences between the water content of the neonatal and adult brain may explain some of the poor diffusion-weighted imaging sensitivity to neonatal ischemia. The neonatal brain has a much higher water content than the adult brain, and thus shows increased water diffusion (16). While ischemia resulting in an area of decreased water diffusion is seen clearly in adults, the same decrease will be relatively less pronounced in the neonate, and may not be as easily discernible.

It is possible that the limited sensitivity of diffusion-weighted imaging might reflect differences in the pathophysiological response of the neonatal brain to ischemia. Global ischemic insults to the neonatal brain preferentially damage particular brain areas. Such ''selective vulnerability'' depends both on the severity and duration of insult and the age of the neonate (18, 19). Severe, acute ischemia commonly causes damage in areas of high metabolic demand, such as the deep gray matter and perirolandic cortex (20). These areas contain a high concentration of excitatory amino acid receptors (21). In contrast, less severe but more prolonged ischemic insults affect the cortical and subcortical watershed regions.

We analyzed our results to assess whether the pattern of injury affected diffusion-weighted imaging sensitivity. Our findings suggested this might be an important factor. While diffusion-weighted imaging was good at detecting isolated cortical injuries, it was poor at detecting damage to the deep gray matter and perirolandic cortex. Furthermore, it underestimated the extent of damage in these subjects. Such gray matter injuries result in a poor neurologic and cognitive outcome (12, 22), and it is important that our chosen imaging method can detect them. It is possible that damage to these areas results in a different cellular response to cortical watershed injuries. Conventional MR appearances are certainly different between the two types of injury. While T1-weighted signal hypointensity, indicating edema, is seen in watershed damage, T1-weighted hyperintensity is seen in deep gray matter injuries (15). The exact origin of the T1 signal changes in the deep gray matter remains unclear, but may reflect hemorrhage (15).

Brain damage resulting from neonatal asphyxia is often called hypoxic-ischemic reperfusion injury, reflecting the importance of both ischemia and arterial reperfusion in eventual damage. The effect and timing of these changes have been observed on diffusion-weighted images of neonatal animals (23, 24). Studies show that a decrease in ADC occurs at two separate time points after injury, with relatively normal values between them. The initial decrease occurs within minutes of insult, and is thought to reflect cellular influx of water, secondary to energy depletion of the cell membrane. Subsequent breakdown of the blood-brain barrier from reperfusion results in accumulation of water in the extracellular space. This increases water diffusion, resulting in a relatively rapid return of ADC to normal values. A second decrease in ADC occurs several days later, thought to reflect resolution of the extracellular edema but persistence of cellular swelling.

We examined the effect of image timing on our results. Once again, we observed possible differences between cortical and deep gray matter injuries. In the cortex, ADC values remained low for the duration of the scanning period, approaching normal values by day 11. In contrast, significantly decreased thalamic ADC values were observed either early (between 2 and 4 days) or late (between 9 and 1 days), with more normal values seen in the times between. While these results are by no means conclusive, they fall more into the pattern suggested by the animal model of neonatal HIE and may reflect possible differences between ischemic insults.

Conclusion

Although diffusion-weighted imaging is a highly sensitive technique for confirming adult cerebral infarction, its ability to detect ischemic damage in neonates with HIE is limited. Diffusion-weighted imaging used either alone or in combination with ADC mapping is insufficient for optimal characterization of HIE based on limited clinical and conventional MR correlation. Furthermore, our results suggest that the sensitivity of diffusion-weighted imaging to HIE may depend on the pattern of injury, with injuries to the cortex being generally well depicted and those in the deep gray matter either underestimated or missed.

References

1. Hill A. **Current concepts of hypoxic-ischemic cerebral injury in the term newborn.** *Pediatr Neurol* 1991;7:317–325

2. van Everdingen KJ, van der Grond J, Kappelle LJ, Ramos LM, Mali WP. **Diffusion-weighted magnetic resonance imaging in acute stroke.** *Stroke* 1998;29:1783–1790
3. Moseley ME, Kucharczyk J, Mintorovitch J, at al. **Diffusion-weighted MR imaging of acute stroke: correlation with T2-weighted and magnetic susceptibility-enhanced MR imaging in cats.** *AJNR Am J Neuroradiol* 1990;11:423–429
4. Baird AE, Benfield A, Schlaug G, et al. **Enlargement of human cerebral ischemic lesion volumes measured by diffusion-weighted magnetic resonance imaging.** *Ann Neurol* 1997;41: 581–589
5. Warach S, Chien D, Li W, Ronthal M, Edelman RR. **Fast magnetic resonance diffusion-weighted imaging of acute human stroke.** *Neurology* 1992;42:1717–1723
6. Warach S, Gaa J, Siewert B, Wielopolski P, Edelman RR. **Acute human stroke studied by whole brain echo planar diffusion-weighted magnetic resonance imaging.** *Ann Neurol* 1995;37: 231–241
7. Burdette JH, Ricci PE, Petitti N, Elster AD. **Cerebral infarction: time course of signal intensity changes on diffusion-weighted MR images.** *AJR Am J Roentgenol* 1998;171:791–795
8. Cowan FM, Pennock JM, Hanrahan JD, Manji KP, Edwards AD. **Early detection of cerebral infarction and hypoxic ischemic encephalopathy in neonates using diffusion-weighted magnetic resonance imaging.** *Neuropediatrics* 1994;25:172–175
9. Robertson RL, Ben-Sira L, Barnes PD, et al. **MR line-scan diffusion-weighted imaging of term neonates with perinatal brain ischemia.** *AJNR Am J Neuroradiol* 1999;20:1658–1670
10. Mercuri E, Cowan F, Rutherford M, Acolet D, Pennock J, Dubowitz L. **Ischaemic and haemorrhagic brain lesions in newborns with seizures and normal apgar scores.** *Arch Dis Child Fetal Neonatal Ed* 1995;73:F67–74
11. Johnson AJ, Lee BC, Lin W. **Echoplanar diffusion-weighted imaging in neonates and infants with suspected hypoxic-ischemic injury: correlation with patient outcome.** *AJR Am J Roentgenol* 1999;172:219–226
12. Barkovich AJ, Hajnal BL, Vigneron D, et al. **Prediction of neuromotor outcome in perinatal asphyxia: evaluation of MR scoring systems.** *AJNR Am J Neuroradiol* 1998;19:143–149
13. Sarnat HB, Sarnat MS. **Neonatal encephalopathy following fetal distress: a clinical and electroencephalographic study.** *Arch Neurol* 1976;33:696–705
14. Stejskal EJT. **Spin diffusion measurements: spin echoes in the presence of a time-dependent field gradient.** *J Chem Phys* 1965; 42:288–292
15. Barkovich AJ, Westmark K, Partridge C, Sola A, Ferriero DM. **Perinatal asphyxia: MR findings in the first 10 days.** *AJNR Am J Neuroradiol* 1995;16:427–438
16. Neil JJ, Shiran SI, McKinstry RC, et al. **Normal brain in human newborns: apparent diffusion coefficient and diffusion anisotropy measured by using diffusion tensor MR imaging.** *Radiology* 1998;209:57–66
17. Lovblad KO, Laubach HJ, Baird AE, et al. **Clinical experience with diffusion-weighted MR in patients with acute stroke.** *AJNR Am J Neuroradiol* 1998;19:1061–1066
18. Myers RE. **Four patterns of perinatal brain damage and their conditions of occurrence in primates.** *Adv Neurol* 1975;10:223–234
19. Barkovich AJ. **MR and CT evaluation of profound neonatal and infantile asphyxia.** *AJNR Am J Neuroradiol* 1992;13:959–972
20. Azzarelli B, Caldemeyer KS, Phillips JP, DeMyer WE. **Hypoxic-ischemic encephalopathy in areas of primary myelination: a neuroimaging and PET study.** *Pediatr Neurol* 1996;14:108–116
21. McDonald JW, Johnston MV. **Physiological and pathophysiological roles of excitatory amino acids during central nervous system development.** *Brain Res Rev* 1990;15:41–70
22. Maller AI, Hankins LL, Yeakley JW, Butler IJ. **Rolandic type cerebral palsy in children as a pattern of hypoxic-ischemic injury in the full-term neonate.** *J Child Neurol* 1998;13:313–321
23. Rumpel H, Nedelcu J, Aguzzi A, Martin E. **Late glial swelling after acute cerebral hypoxia-ischemia in the neonatal rat: a combined magnetic resonance and histochemical study.** *Pediatr Res* 1997;42:54–59
24. Tuor UI, Kozlowski P, Del Bigio MR, et al. **Diffusion- and T2-weighted increases in magnetic resonance images of immature brain during hypoxia-ischemia: transient reversal posthypoxia.** *Exp Neurol* 1998;150:321–328